Fizika Nizkikh Temperatur, 2007, v. 33, Nos. 6/7, p. 798–804

Heat transfer in crystalline clathrate hydrates at low temperatures

A.I. Krivchikov, O.A. Korolyuk, and O.O. Romantsova

B. Verkin Institute for Low Temperature Physics and Engineering of the National Academy of Sciences of Ukraine
47 Lenin Ave., Kharkov 61103, Ukraine
E-mail: krivchikov@ilt.kharkov.ua

Received October 20, 2006

The experimental results on the thermal conductivity $\kappa(T)$ of crystalline Xe, CH_4, and THF clathrate hydrates have been analyzed. In a wide region of temperatures above 2 K, $\kappa(T)$ exhibits a behavior typical of disordered solids, which depends weakly on their chemical composition, crystalline structure and microstructure. The results are discussed in the context of phenomenological models of phonon scattering by local modes. It has been found that the Xe clathrate has a feature unusual for glasses, namely, $\kappa(T)$ decreases almost two-fold as the temperature increases from 50–100 K. The behavior of $\kappa(T)$ is presumably determined mainly by the strong phonon scattering on water molecules.

PACS: **66.70.+f** Nonelectronic thermal conduction and heat-pulse propagation in solids; thermal waves;
63.20.–e Phonons in crystal lattices;
63.20.Pw Localized modes;
63.50.+x Vibrational states in disordered systems.

Keywords: thermal conductivity, proton disorder, soft potential model, crystalline structure, microstructure.

Introduction

Clathrate hydrates are ice-like solids formed of a nonstoichiometric mixture of water and low-molecular gases or liquids. In clathrate hydrates the water molecules linked by hydrogen bound form an open cage with numerous polyhedral voids capable of housing guest molecules of other chemically low-active or inactive substances, including inert gases, O_2, CH_4, CO_2, Cl_2, etc. Most gases (Ar, Kr, Xe, O_2, N_2, CO_2, CH_4, H_2S and so on) can form hydrates under moderate excess pressures at room temperature. Crystalline hydrates with relatively large guest molecules (e.g. tetrahydrofuran and ethylene oxide) can be synthesized easily from a liquid solution.

Under natural conditions, clathrate hydrates were discovered as clathrate hydrates of methane in vast deposits at the world ocean bottom and in the Earth's interior or as hydrocarbon clathrates plugging the insides of gas and oil pipelines in the Arctic latitudes. Gas hydrates can exist in a relatively narrow domain of thermodynamic stability so that disturbance of the equilibrium conditions can lead to their decomposition and the liberation of gas. In laboratories, gas hydrates are obtained in the form of fine disperse powders by saturation of fine crystals of ice with gas under elevated pressure.

Despite quite intense research on clathrate hydrates, there still are open questions about their microstructure, formation, decomposition and dynamic properties. The first measurement of the thermal conductivity of clathrate hydrates dates back to 1981 [1]. It was found that the thermal conductivity of clathrates differed drastically from that of ice both in magnitude and temperature dependence. Later on, different research groups [2–4] investigated the thermal conductivity of clathrate hydrates prepared from a solution of water and a low-molecular liquid (55–250 K). The thermal conductivity of CH_4 hydrate was measured at rather high temperatures $T > 235$ K [5,6]. The investigation of the thermal conductivity of tetrahydrofuran (THF) hydrate was performed at 15–100 K [7], but those results were underestimated and showed rather poor agreement with other thermal conductivity data of hydrates. Nevertheless, the authors emphasized a glass-like behavior of the thermal conductivity.

Recently, the thermal conductivity has been measured on gas hydrates of methane [8], xenon [9] and tetrahydrofuran [10] in a wide temperature region. These hydrates have different types of clathrate structure. The $\kappa(T)$

curve of CH_4 and THF hydrates at T = 2–220 K demonstrates a weak dependence on the type of guest molecules or clathrate structure and exhibits a behavior typical of amorphous or disordered solids. The Xe hydrate has an unusually strong anomalous feature in the region 55–95 K.

In this study the experimental results on the low temperature thermal conductivity of clathrate hydrates of Xe, CH_4 and THF have been analyzed on the basis of two theoretical approaches: the soft potential model and the resonance scattering model. The clathrates were chosen so that we could take into account basically different factors that could influence the heat transfer at low temperatures. The guests of approximately similar size were Xe atoms and symmetrical CH_4 molecule (quantum rotators) which have rotational degrees of freedom.

The Xe and CH_4 hydrates have identical crystalline cubic type I ($Pm3n$, a = 12 Å) structures in which «guests» occupy all cavities of the clathrate. The C_4H_8O (THF) molecule is larger than the CH_4 molecule. The THF based clathrate hydrate ($THF{\cdot}17H_2O$) has a crystalline cubic type II structure ($Fd3m$, a = 17.1 Å) in which only large cavities can be occupied by the «guest».

Since many gas hydrates have a porous submicron structure, the ordinary methods cannot ensure accurate measurement of thermal conductivity. In this paper we present a comparative qualitative analysis of the temperature dependence of the thermal conductivity for Xe, CH_4 and THF hydrates, discuss the thermal conductivities calculated within current theoretical models and consider the problems connected with the measurement of thermal conductivities of clathrate hydrates.

Experiment

Thermal conductivities of clathrate hydrates of CH_4, Xe and THF [8–10] were measured in a wide temperature region above 2 K by the steady-state heat flow technique [11] using the same setup.

The samples of clathrate CH_4 and Xe hydrates were fine disperse powders, which decompose into gas and ice at room temperature. It is therefore basically impossible to measure their true thermal conductivity that corresponds to the thermal conductivity of a homogeneous continuous solid. Instead, we measured the effective thermal conductivity $\kappa_{eff}(T)$ of the sample in the medium of heat-exchanging He gas. The sample occupied only a part of the volume of the measuring container. The rest of the space was filled with He gas under reduced pressure. The filling density of the sample was $\eta = V_s/V$, ($\eta < 1$), where V_s is the sample volume, V is the volume of an empty container. The true thermal conductivity $\kappa(T)$ corresponding to the thermal conductivity of a homogeneous substance can be deduced from $\kappa_{eff}(T)$ using simple models of heat transfer in inhomogeneous media disregarding for the thermal resistance of the boundary of the two media. The temperature dependencies calculated for Xe and CH_4 hydrates within certain models are shown in Figs. 1 and 2. The true thermal conductivity was extrated from $\kappa_{eff}(T)$ using the model of parallel layers. The thermal conductivity of granular materials is commonly described by simple Eq. (1) relating κ_{eff} and κ [12–14]:

$$\kappa_{eff} = \kappa{\cdot}\eta + \kappa_{He}\,(1 - \eta), \qquad (1)$$

where κ_{He} is the thermal conductivity of the heat exchange ^{4}He gas. However, this equation is empiric and does not allow for the structure of the material and the thermal contact resistance at the grain boundaries. Recently [15] the composite thermal conductivity of a porous methane hydrate sample was determined as a function of density. Mixing models (i.e., arithmetic, harmonic, geometric mean, and square root models) were compared with estimated composite thermal conductivity determined by inverse modeling. The results of the arithmetic mean model showed the best agreement with the estimated composite thermal conductivity [15]. To test its applicability to our case, we compared the κ values that were calculated for a homogeneous material using Eq. (1) from the κ values measured on two samples of Xe hydrate which differed in preparation technology, grain size, and filling density η. The two samples had significantly different contact resistances and different contributions of the heat exchange gas to the heat transport. The thermal conductivities calculated by Eq. (1) for the homogeneous materials of the two different samples of Xe hydrate coincide within experimental error. A similar testing was performed for the samples of CH_4 hydrates. The agreement was good again. The other models (2)–(6) provide worse agreement.

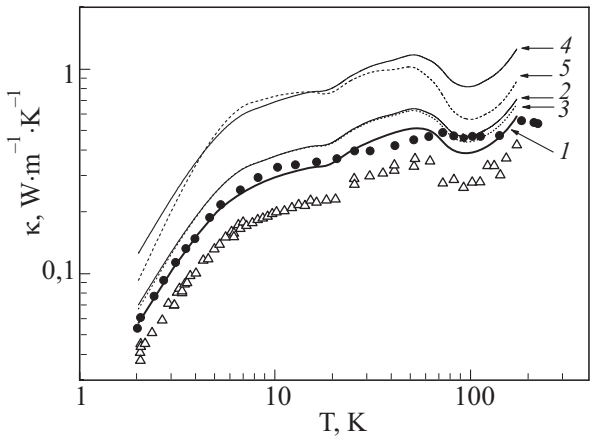

Fig. 1. The temperature dependencies for the THF and CH_4 hydrates. The measured effective thermal conductivity of CH_4 hydrate, the density of filling of the container with the sample is η =0.65 (△); the thermal conductivity of CH_4 hydrate (solid substance) calculated by different models: parallel layers model (arithmetic mean model) [12–15] (*1*); Jagjiwanram model [16] (*2*); Adler model [17] (*3*); Rayleigh model [12] (*4*), geometric model [18] (5). For comparison, the thermal conductivity of THF clathrate hydrate is shown (●), η = 1.

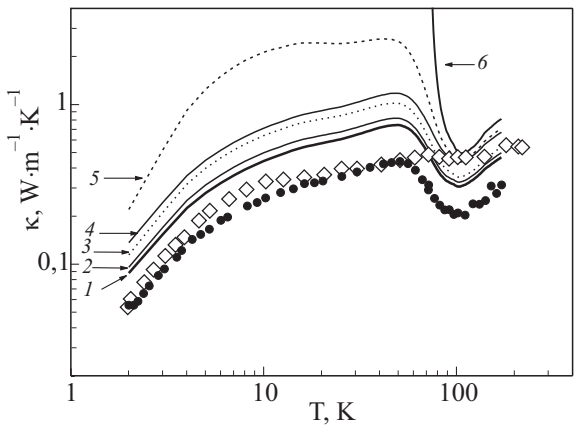

Fig. 2. The temperature dependencies for the THF and Xe hydrates. The measured effective thermal conductivity of Xe hydrate, the filling density of the container is η = 0.56 (●). The thermal conductivity of Xe hydrate (solid substance) calculated by different models: parallel layers model (arithmetic mean model) [12–15] (*1*); Jagjiwanram model [16] (*2*); Adler model [17] (*3*); Rayleigh model [12] (*4*), geometric model [18] (*5*); Maxwell model [19] (see the brief description in the Appendix) (*6*). For comparison, the thermal conductivity of THF clathrate hydrate is shown (◊), η = 1.

The samples of clathrate Xe hydrate were obtained from different sources and differed in preparation technology. In the $Xe{\cdot}5.9H_2O$ samples (the material provided by the National Research Council of Canada), 98% of clathrate cavities were filled with Xe atoms, the grain sizes were 1–3 μm [9]. In the $Xe{\cdot}6.2H_2O$ samples (the material from Gцttinger Zentrum Geowissenschaften, University of Gцttingen, Germany) [9] 92% of clathrate cavities were occupied by Xe atoms, the grain size was 0.1–1 mm.

The $CH_4{\cdot}5.75H_2O$ hydrate, also produced at the Göttinger Zentrum Geowissenschaften, University of Göttingen in Germany [8], had grain sizes 2–3 mm and ~1 mm. The clathrate cavities were 100% filled with CH_4 molecules.

Under the normal conditions, tetrahydrofuran hydrate ($THF{\cdot}17H_2O$) is a liquid with the crystallization temperature 278.15 K. The $THF{\cdot}17H_2O$ sample was prepared by dissolving pure (99.9%, ACROS Organics) tetrahydrofuran C_4H_8O (THF) in double-distilled water. THF and water were mixed in the molar ratio 1:16.9 [10]. The liquid solution was poured into the measuring container at room temperature. The container was then cooled, and a homogeneous crystalline sample was grown following the accepted procedure (cooling rate of 5.7 K/min, crystallization in the space between two thermometers took 7 min, the distance between the thermometers was 12.3 mm) [10].

The thermal conductivity κ(*T*) of Xe and CH_4 gas hydrates derived from $\kappa_{eff}(T)$ and the thermal conductivity of THF are shown in Fig. 3. The κ(*T*) values for the samples of Xe gas hydrates [9] coincided. The same holds for the thermal conductivity of CH_4 hydrate sample [8]. At high (170 K) temperatures the thermal conductivities of these hydrates differ by only 20%. The κ(*T*) curve for the Xe hydrate exhibits a distinct minimum at T ≈ 100 K, a growth with lowering temperature and a maximum at $T \approx 51$ K. Below 50 K the temperature dependence of the thermal conductivity of Xe hydrate is rather smooth: the thermal conductivity decreases with lowering temperature. The κ(*T*) curve of CH_4 hydrate behaves similarly. There is a minimum and a maximum at the same temperatures, but they are less pronounced than in the case of Xe hydrate. The figure also illustrates the thermal conductivity of THF hydrate. Although the THF hydrate is a homogeneous crystalline sample with a cubic type II structure, below 25 K its κ(*T*) values practically coincide with those of CH_4 hydrate. The thermal conductivity of THF hydrate increases with temperature. At 170 K the thermal conductivities of the three hydrates become close. The κ(*T*) curves of the hydrates investigated below 50 K have shapes that are typical of glasses: at liquid helium temperatures they approach a quadratic law ($\sim T^2$) and become weakly on temperature dependent when it starts rising. There are several reasons for this «glassy» behavior.

1. It can be connected with structural disorder. The frozen orientational disorder can develop in a crystalline clathrate due to proton disorder in the lattice consisting of H_2O molecules and the orientational disordering of the guest molecules in the clathrate cavities [4]. The glass transition in clathrate hydrates was observed [20] near $T = 85$ K and was followed by a small heat capacity jump.

Since the interaction between host and guest molecules is rather weak, guest molecules can be dynamically disordered at high temperatures and statically disordered at low temperatures. We can expect that the heat is transported mostly through the strongly bound H_2O molecules

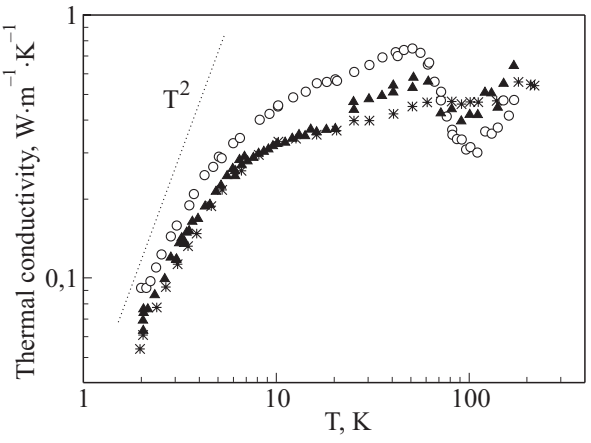

Fig. 3. Thermal conductivity of clathrate hydrates: THF hydrate (✳), CH_4 hydrate (▲), Xe hydrate (○).

in the host lattice, while the guest molecules act as point defects. The phonons are scattered on the guest molecules and on the lattice distortions associated with the proton disorder. However, because of the weak host–guest interaction, the guest molecules are incapable of ensuring the intensive phonon scattering necessary for the glassy behavior of the thermal conductivity.

2. It is assumed that the low-frequency rattling vibration of guest molecule in the cavity interacts with the host lattice [21]. This leads to a resonance scattering of thermal phonons, which can be another factor responsible for the glassy behavior of the thermal conductivity. Although this model is in conflict with the previous assumption (weak guest-host interaction), it can describe the results for all clathrate hydrates. There are, however, reliable experimental data obtained, NRIXS (nuclear resonant inelastic x-ray scattering spectroscopy), IINS (incoherent inelastic neutron scattering) investigations and molecular dynamic simulations, which show that the glass behavior of the thermal conductivity of clathrates is a consequence of a strong guest–host interaction [21].

3. This assumption concerns type I and type II clathrate hydrates with large unit cells. In such hydrates the phonon mean free path is limited by the size of the unit cell. As shown by Dharma–Wardana [22], thermal conduction acquires to glass – like behavior if the unit cell has a large number of oscillatory modes. The mean free path is assumed to be temperature independent, being about 12 Å [7] (the size of the unit cell).

Figure 4 illustrates the temperature dependence of the phonon mean free path for the investigated clathrate hydrates. It was calculated from our thermal conductivities within the Debye model using the simple gas kinetic equation

$$\kappa(T) = \nu\, l C_{\rm ph}/3,$$

where $C_{\rm ph}$ is the phonon heat capacity, l is the phonon mean free path, and ν is the mean sound velocity. The dash-dotted, dash, and dotted lines show lattice parameter values for structures I (a = 12 Å) and II (a = 17.3 Å), and the mean distance between oxygen atoms (a = 2.78 Å) that form the cage in the clathrate structure of THF hydrate lattice, respectively. It is seen that the mean free path of the phonons is strongly temperature dependent, i.e. assumption 3 is wrong. At low temperatures the phonon mean free path exceeds considerably the spacing between oxygen atoms and the motion of phonons is «ballistic». As the temperature increases, the mean free path decreases. Above 100 K it becomes practically temperature independent and nearly equal to the spacing between the oxygen atoms. This picture is observed for all clathrate hydrates investigated. In this temperature region the phonon motion is diffusive (Ioffe–Riegel regime). The phonon – based concept is inapplicable at such low l-values, and the energy is exchanged directly between

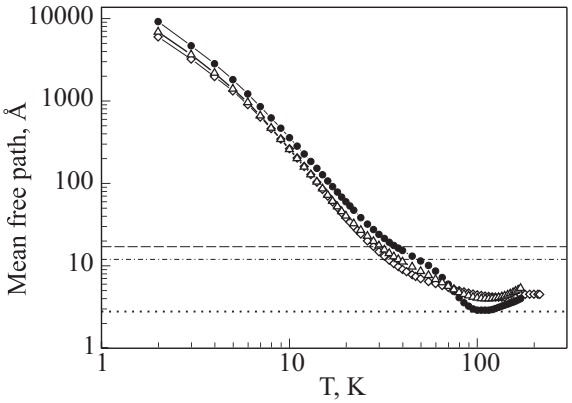

Fig. 4. Temperature dependence of the phonon mean free path calculated from the thermal conductivity data for THF hydrate (◊), Xe hydrate (●), CH_4 hydrate (△). The mean spacing between O atoms in the THF hydrate lattice is shown by a dotted line; lattice parameter values of clathrate structures I (a = 12 Å) and II (a = 17.3 Å) are shown by lines (-·-·-) and (----), respectively.

the neighboring molecules. We can thus distinguish two temperature regions in which different heat transfer mechanisms are in operation. The crossover from ballistic to diffusive require occurs in the interval from about 50 to 100 K, where both heat exchange mechanisms work. The contribution of phonon flow to the heat depends on the phonon wavelength.

Discussion

The results on the thermal conductivity of clathrate Xe, CH_4, THF hydrates were analyzed within the Debye model. Let τ_G be is the characteristic relaxation time due to resistive processes of phonon scattering, which can be described using two different approaches, the soft potential model or the resonance scattering. We took into consideration the fact that τ_G is not smaller than $\tau_{\rm min} = 2/\omega$. At high temperatures the localized excitations in hydrates are fully activized and the mean free path of phonons is therefore nearly constant.

It is expected that the guest molecule tunneling between two minima in the hydrate cavities starts to play an important role at low temperatures [7]. To calculate τ_G^{-1}, we used the phenomenological model of soft potentials, which is well known as a tunnel model describing the properties of glasses at $T \sim 1$ K [23,24]:

$$\tau_G^{-1} = \pi\, \overline{C}\omega \tanh\left(\frac{\hbar\omega}{2k_B T}\right) + \pi\overline{C}\omega\left(\frac{T}{W}\right)^{3/4} + \frac{\pi\overline{C}\omega}{6\sqrt{2}}\left(\frac{\hbar\omega}{W}\right)^3, \quad (2)$$

where $\overline{C}$ and W are the parameters of the model. The most relevant parameters are the dimensionless parameter $\overline{C}$ and the characteristic energy W [24,25]. The phonon scat-

tering (τ_G^{-1}) consist of tunnel states, classical relaxors and soft quasiharmonic vibrations. The energy W was calculated from the maximum temperature T_{max} of the temperature dependence of $\kappa(T)/T$: $W \approx 1.6\, k_B T_{max}$ [24].

The glass-like behavior of the thermal conductivity of clathrate hydrates can be caused by strong coupling between the rotational and translational motions of guest molecule and the lattice vibrations [7,26]. The phenomenological model of resonance scattering yields [7]:

$$\tau_G^{-1} = D\frac{\omega^2}{(\omega^2 - \omega_0^2)^2}, \qquad (3)$$

where D is the scattering parameter depending both on the number of guest molecules and on the lattice guest coupling; ω_0 is the vibration frequency of the guest particles responsible for resonance scattering.

The results of fitting of the thermal conductivities of THF and Xe hydrates within the two models, Eqs. (2) and (3), are shown in Fig. 5. The fitting parameters are given in Table 1. There are two distinct temperature regions in which the thermal conductivity is described by different models. At low temperatures the motion of phonons is ballistic and the thermal conductivity of the THF and Xe hydrates can be described well by both models. At high temperatures the phonon mean free path is comparable with the spacing between oxygen atoms in the hydrate lattice and the thermal conductivity of the Xe hydrate is poorly described by both models. The soft potential model consistently describes the thermal conductivity of the THF hydrate in the whole temperature region. By contrast, the resonance scattering model can describe the thermal conductivity only at low temperatures.

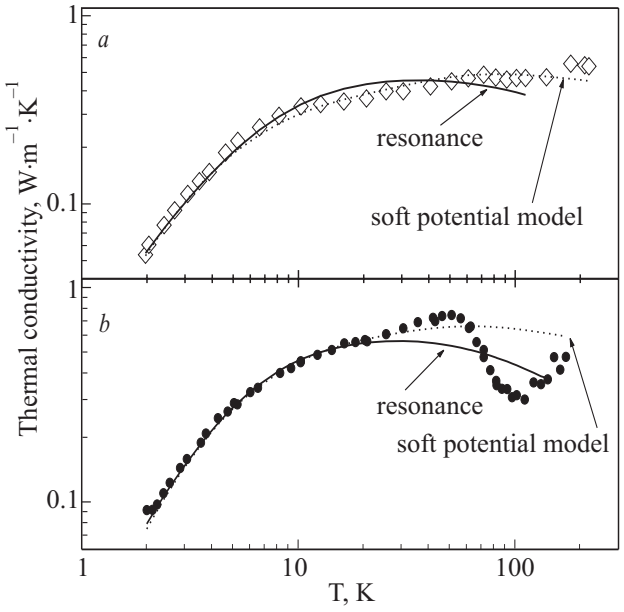

Fig. 5. Thermal conductivity of THF (*a*) and Xe (*b*) hydrates described by the models of resonance scattering (——) and soft potentials (-----).

Table 1. Parameters to fit the thermal conductivity of CH_4, Xe and THF hydrate. The average sound velocities for CH_4 and Xe hydrates are calculated from longitudinal sound velocities of [27]. Θ_D is calculated within the Debye model using the average sound velocities

Sample	Θ_D, K	v, m/s	ω_0, K	D, s^{-3}	W, K	$\overline{C}$
CH_4 hydrate	190	2023	58 [27]	$8.1\cdot10^{36}$	5	$0.311\cdot10^{-3}$
THF hydrate	171	1871 [28]	58	$8.4\cdot10^{36}$	6	$0.486\cdot10^{-3}$
Xe hydrate	140	1485	46 [29]	$1.9\cdot10^{36}$	6	$0.426\cdot10^{-3}$

The heat capacity data for the THF hydrate yield Θ_D = = 198 K [7,30], which is 27 K higher than our result. However, this discrepancy between the Debye temperatures does not affect the fitting curve below 20 K. The frequency of localized vibrations, in large cavities, ω_0, is 3.9 meV (45.24 K) for Xe [27,31], which is consistent with the corresponding value at 46 K; for the THF hydrate we took ω_0 equal to that of the CH_4 hydrate. The fitted frequency-independent tunneling strength $\overline{C}$ is within the interval 10^{-4} – 10^{-3}, which agrees with the assumption of the *universal* character of this parameter for different amorphous bodies [25].

Conclusions

A complex analysis of experimental results on the effective thermal conductivity of the CH_4 and Xe clathrate hydrates and the thermal conductivity of the clathrate THF hydrate at T = 2–170 K shows that this class of substances can be considered as crystals possessing the properties of a glass. The results are in good quantitative agreement with theoretical models used to describe structural glasses. The following glass-related features were observed in the behavior of $\kappa(T)$: a T^2 — dependence below 3 K, a smeared «plateau» $\kappa(T) \sim T^n$ with n = 0.3 at T 6–50 K and a smooth growth of $\kappa(T)$ typical of the «diffusive» regime of heat transfer. It is found that the $\kappa(T)$ curve of the Xe clathrate has a minimum at $T \approx 100$ K, followed by a growth at lower temperatures and a maximum at $T \approx 50$ K, which is unusual for glasses

Appendix

There are several models that can be used to extract the true thermal conductivity $\kappa(T)$ corresponding to that of a pure substance from $\kappa_{eff}(T)$ measured on two-phase systems (CH_4 and Xe hydrates and the exchange gas, in our case). Some of the models are considered below.

1. The simple relation given by Eq. (1) for powders [12–15] relates the effective and true thermal conductivities, assuming that the heat flow is parallel to parallel layers of the two components (hydrate, exchange gas).

In our case κ_{eff}, κ, κ_{He} are the measured effective thermal conductivity of the hydrate, the true thermal conductivity, and the thermal conductivity of the gas, respectively; η is the filling ratio of the container with the sample. The lines in Figs.1 and 2 describe the thermal conductivities of powder gas hydrates of CH_4 and Xe using this model.

2. Theoretical model (2) [16] was developed for real two-phase systems. The model assumes a linear heat flow in a three-dimensional cubic system of ellipsoidal particles. The true and effective thermal conductivities are related as

$$\kappa_{eff} = \frac{\kappa_{He}[(\kappa-\kappa_{He})\sqrt{\pi/6}\eta^{1/2}+\kappa_{He}]}{[(1-\sqrt{6/\pi}\eta^{1/2})(\kappa-\kappa_{He})(\sqrt{\pi/6}\eta^{1/2})]+\kappa_{He}]}.$$

The permissible interval of the filling density in this model [16] is $0 < \eta < 0.52$. In our experiments, the filling ratio measuring container were $\eta = 0.65$ (CH_4 hydrate) and $\eta = 0.562$ (Xe hydrate). In Figs. 1 and 2, model (2), the filling density was the highest: $\eta = 0.52$.

3. In the Adler model [17] developed to describe the electric conductivity of disordered systems, the effective and true thermal conductivities are related as

$$\kappa_{eff} = [\eta\kappa^{1/2} + (1-\eta)\kappa_{He}^{1/2}]^2.$$

4. The Rayleigh model [12] is applied to heterogeneous solids (spheres built into intersections of the cubic lattice):

$$\frac{\kappa_{eff}}{\kappa} = 1 + \frac{3\eta}{\left(\frac{\kappa_{He}+2\kappa}{\kappa_{He}-\kappa}\right) - \eta + 1.569\left(\frac{\kappa_{He}-\kappa}{3\kappa_{He}-4\kappa}\right)\eta^{10/3}+\ldots}.$$

5. In the geometrical model (5) [18] (for filled polymers) the effective and true thermal conductivities are related as

$$\kappa_{eff} = \kappa^{\eta}\kappa_{He}^{1-\eta}$$

6. Maxwell [19] obtained the following relation for the effective and true thermal conductivities of randomly located and non–interacting homogeneous spheres in a homogeneous medium (6):

$$\kappa_{eff} = \kappa_{He}\frac{\kappa+2\kappa_{He}+2\eta(\kappa-\kappa_{He})}{\kappa+2\kappa_{He}-\eta(\kappa-\kappa_{He})}.$$

We used the model of parallel layers (arithmetic mean model) (1) to deduce the true thermal conductivity from the measured effective thermal conductivity.

The study was partially supported with a Grant of President of Ukraine for young scientists engaged in scientific research (GP/F13/0037).

We thank Prof. Vadim Manzhelii, Prof. Werner Press, and Prof. Javier Bermejo for fruitful discussions.

1. R.G. Ross, P. Andersson, and G. Backström, *Nature* **290**, 322 (1981).
2. P. Andersson and R.G. Ross, *J. Phys.* **C16**, 1423 (1983).
3. N. Ahmad and W.A. Phillips, *Solid State Commun*. **63**, 167 (1987).
4. O.P. Andersson and H. Suga, *J. Phys. Chem. Solids* **57**, 125 (1996).
5. J.G. Cook and D.G. Leaist, *Geophys. Res. Lett*. **10**, 397 (1983).
6. D. Sloan, Jr., *Clathrate Hydrates of Natural Gases,* Basel, Marcel Dekker, N.Y. (1990).
7. J.S. Tse and M.A. White, *J. Phys. Chem*. **92**, 5006 (1988).
8. A.I. Krivchikov, B.Ya. Gorodilov, O.A. Korolyuk, V.G. Manzhelii, H. Conrad, and W. Press, *J. Low Temp. Phys.* **139**, 693 (2005).
9. A.I. Krivchikov, B.Ya. Gorodilov, O.A. Korolyuk, V.G. Manzhelii, O.O. Romantsova, H. Conrad, W. Press, J.S. Tse, and D.D. Klug, *Phys. Rev.* **B73**, 064203 (2006).
10. A.I. Krivchikov, V.G. Manzhelii, O.A. Korolyuk, B.Ya. Gorodilov, and O.O. Romantsova, *Phys. Chem. Chem. Phys.* **7**, 728 (2005).
11. A.I. Krivchikov, B.Ya. Gorodilov, and O.A. Korolyuk, *Prib. Tekh. Eksp.* **48**, 1 (2005).
12. A. Missenard, *Conductivite Thermique des Solides, Liuides, Gaz et de Leurs Melanges*, Editions Eyrolles, Paris (1965).
13. G.N. Dulnev and Yu.P. Zarichnyak*, Heat Conductivity of Mixtures and Composite Materials,* Energiya, Moscow (1974).
14. Ye.Ya. Litovsky and N.A. Puchkelevich, *Thermal Properties of Heat-Resistant Materials,* Metallurgiya, Moscow (1982).
15. A. Gupta, T.J. Kneafsey, G.J. Moridis, Y. Seol, M. Kowalsky, and E.D. Sloan, Jr., *J. Phys. Chem*. **B110,** 16384 (2006).
16. Jagjiwanram and Ramvir Singh, *Bull. Matter. Sci*. **27**, 373 (2004).
17. D. Adler, L.P. Flora, and S.D. Senturia, *Solid State Commun.* **12**, 9 (1973).
18. Y. Agari and T. Uno, *J. App. Polym. Comp. Sci.* **32***,* 5705 (1986).
19. C. Maxwell, *A Treatise on Electricity and Magnetism*, Dover, New York (1954), ch. 9.
20. O. Yamamuro, M. Oguni, T. Matsuo, and H. Suga, *J. Phys. Chem. Solids* **49**, 425 (1988).
21. S. Tse, D.D. Klug, J.Y. Zhao, W. Sturhahn, E.E. Alp, J. Baumert, C. Gutt, M.R. Johnson, and W. Press, *Nature Mater.* **4**, 917 (2005).
22. C. Dharma-Wardana, *J. Phys. Chem*. **87**, 4145 (1983).
23. U. Buchenau, Yu.M. Galperin, V.L. Gurevich, D.A. Parchin, M.A. Ramos, and H.R. Schober, *Phys. Rev.* **B46**, 2798 (1992).
24. M.A. Ramos and U. Buchenau, *Phys. Rev*. **B55**, 5749 (1997).
25. O. Pohl, X. Liu, and E. Thompson, *Rev. Mod. Phys*. **74**, 991 (2002).
26. J.S. Tse, V.P. Shpakov, V.V. Murashov, and V.R. Belosludov, *J. Chem. Phys*. **107**, 9271 (1997).

27. J. Baumert, C. Gutt, V.P. Shpakov, J.S. Tse, M. Krisch, M. Müller, H. Requardt, D.D. Klug, S. Janssen, and W. Press, *Phys. Rev.* **B68**, 174301 (2003).
28. M. Bathe, S. Vagle, G.A. Saunders, and E.F. Lambson, *J. Mater. Sci. Lett*. **3**, 904 (1984).
29. J.S. Tse, V.P. Shpakov, V.R. Belosludov, F. Trouw, Y.P. Handa, and W. Press, *Europhys. Lett.* **54**, 354 (2001).
30. M.A. White and M.T. Maclean, *J. Phys. Chem*. **89**, 1380 (1985).
31. C. Gutt, J. Baumert, W. Press, J.S. Tse, and S. Janssen, *J. Chem. Phys*. **116**, 3795 (2002).